

Cite this: *RSC Adv.*, 2018, 8, 25575

## P1c peptide decorated liposome targeting $\alpha v \beta 3$ -expressing tumor cells *in vitro* and *in vivo*

Wei Xu,<sup>†a</sup> Xuejiao Yan,<sup>†ab</sup> Naifeng Liu<sup>\*acd</sup> and Guoqiu Wu<sup>id\*ac</sup>

Integrin  $\alpha v \beta 3$  is a promising target for integrin-rich tumor and neovascular. In the present study, we prepared a doxorubicin (DOX)-loaded liposome of which the surface was decorated with PEG and a novel  $\alpha v \beta 3$  targeting peptide of P1c. The *in vitro* targeting efficiency was evaluated in  $\alpha v \beta 3$ -positive (U87MG) and -negative (MCF-7) tumor cells by flow cytometry and laser confocal scanning microscopy. The *in vivo* therapeutic effects were evaluated in the glioblastoma U87MG-tumor bearing mouse model. The results indicated that the prepared liposomes showed mean sizes of 131.2 and 128.4 nm in diameter for P1c-modified targeting liposomes (P1c-DOXL) and non-targeting liposomes (DOXL), respectively. The DOX encapsulation efficiencies were more than 95% in both types of liposomes. The conjugation ratio for P1c decoration was 66.8%. The flow cytometry and confocal laser-scanning microscopy experiments consistently showed that the intracellular fluorescence intensity of the P1c-modified targeted liposome group was stronger than that of the non-targeted liposome group ( $P < 0.05$ ) in U87MG cells. *In vivo* results revealed that compared with DOX or DOXL treatment, P1c-DOXL dramatically reduced tumor growth ( $P < 0.05$ ) and tumor angiogenesis while much lower hepatotoxicity was observed. P1c-modified targeting liposome exhibited sustained release, enhancing the antitumor effect of DOX through targeting tumor cells and neovascular where integrin  $\alpha v \beta 3$  was overexpressed. The results indicated that P1c might be promising for active targeting delivery in cancer therapy.

Received 11th June 2018

Accepted 8th July 2018

DOI: 10.1039/c8ra05014g

rsc.li/rsc-advances

## Introduction

Liposomes have been extensively utilized as drug delivery carriers for cancer therapy.<sup>1–3</sup> Long-circulating liposomes, produced by modification with poly(ethylene glycol) (PEG) are able to passively accumulate in tumors *via* the enhanced permeability and retention (EPR) effect, in which case they are usually called “sterically stable liposomes” (SSL).<sup>4–7</sup> Hydrogenated soybean phosphatidylcholine (HSPC) and cholesterol is a common material to prepare liposomes.<sup>8,9</sup> Active targeting can be achieved by modification of sterically stable liposomes with various ligands, such as antibodies, peptides, folic acid, or transferrin, to enhance distribution in tumor sites and reduce side effects to normal tissues.<sup>10–17</sup>

Integrins are a family of cell surface receptors that consist of noncovalently associated  $\alpha$  and  $\beta$  subunits.<sup>18</sup> They can primarily mediate interactions of cells with the extracellular matrix.<sup>19</sup>  $\alpha v \beta 3$ , one member of integrins, seems to play a critical role in

regulating tumor growth, metastasis, and angiogenesis. It was reported that although integrin  $\alpha v \beta 3$  was significantly up-regulated in sprouting tumor vessels and solid tumor cells of various origins, it was only minimally expressed in quiescent blood vessels and normal cells.<sup>20,21</sup> Previous studies demonstrated that integrin  $\alpha v \beta 3$  antagonists, such as arginine-glycine-aspartic acid (RGD) peptides conjugated drug delivery system targeting  $\alpha v \beta 3$  has been developed for target cancer therapy and diagnostics.<sup>22–28</sup>

P1c is a novel peptide (CIRTPKISKPIKFELSG, Chinese patent no. ZL 2009 10025 731.0) derived from human connective tissue growth factor (CTGF). In our previous study, we find that P1c could specifically bind to human integrin  $\alpha v \beta 3$ . After coupled with ultrasuperparamagnetic iron oxide particles (USPIOs), P1c had been successfully applied in magnetic resonance imaging (MRI) of human primary liver cancer (Bel 7402) that up-regulated  $\alpha v \beta 3$  expression.<sup>29</sup> In the present study, we investigated the targeting potential of P1c after conjugated on the surface of liposome.

## Materials and methods

### Materials

Hydrogenated soybean phosphatidylcholine (HSPC), cholesterol, 1,2-dioleoyl-*sn*-glycero-3-phosphoethanolamine-*N*-[methoxy(polyethylene glycol)-2000] (DSPE-PEG2000), and

<sup>a</sup>Medical School of Southeast University, Nanjing 210009, China<sup>b</sup>The Affiliated Changzhou No. 2 People's Hospital of Nanjing Medical University, Changzhou 213000, China<sup>c</sup>Center of Clinical Laboratory Medicine of Zhongda Hospital, Southeast University, Nanjing 210009, China. E-mail: nationball@163.com; Tel: +86-25-83272355<sup>d</sup>Department of Cardiology, Zhongda Hospital, Southeast University, Nanjing 210009, China. E-mail: Liunf@seu.edu.cn; Tel: +86-25-83272001

† These authors contributed equally to this work.



functional DSPE-PEG2000-COOH-NHS were purchased from Shanghai A.V.T Pharmaceutical LTD (Shanghai, China). P1c peptide was obtained from Science Peptide Biological Technology Co., LTD (Shanghai, china). Doxorubicin hydrochloride was purchased from Dalian Meilun Biology Technology Co., LTD (Dalian, China). Dulbecco's Modified Eagle's Medium (DMEM) and fetal bovine serum (FBS) were from Life Technologies, Inc (Grand island, NY). The human glioblastoma cells (U87MG) and human breast cancer cells (MF-7) were obtained from Cell-bio Ins, SAC (Shanghai, China). Cell Counting Kit-8 (CCK-8) was purchased from Sigma-Aldrich (St. Louis, MO, USA). Anti-human  $\alpha\beta 3$  monoclonal antibody (mAb) was purchased from R&D Systems (Minneapolis, MN, USA).

### Synthesis of P1c-PEG2000-DSPE

The P1c-PEG-DSPE conjugate was synthesized according to the manufactory's instruction. In brief, DSPE-PEG2000-COOH-NHS was dropped into the MES buffer (pH 8.0) containing 1 mg mL<sup>-1</sup> P1c peptide (peptide : DSPE-PEG2000-COOH 1.1 : 1 mol mol<sup>-1</sup>) and stirred for 24 h at room temperature. The mixture was ready for use in the liposomes preparation.

### Preparation of liposomes

A total amount of 5 mg liposomes composed of HSPC and cholesterol (molar ratio: 2/1) was prepared by the lipid film hydration method. After evaporation overnight, the lipid film was hydrated with 1 mL, 250 mM ammonium sulfate for 30 minutes at 60 °C followed by sonication (400 W, 30 min). The liposome suspensions were then applied to dialysis (MW cut off 10 kDa) against a 200-fold volume of 10% sucrose solution overnight to establish a transmembrane NH<sub>4</sub><sup>+</sup> gradient followed

by extruded through a polycarbonate filter of 0.22  $\mu\text{m}$  for homogenization. An amount of 0.5 mg DOX dissolved in 1 mL 10% sucrose solution was mixed with the liposomes and incubated for 30 minutes at 60 °C. DSPE-PEG or P1c-PEG-DSPE was then added by 5% of the total lipid weight and incubated for another 30 min to prepare DOXL or P1c-DOXL, respectively. The liposomes were finally dialyzed extensively (MW cut off 10 kDa) against PBS (pH 7.4) for 24 h to remove free DOX or P1c.

### Characterization of liposomes

The mean size, polydispersity (PDI) and zeta potential of the prepared liposomes were determined using a Zetasizer Nano ZS ZEN3600 instrument (Malvern Instruments LTD., Worchester-shire, UK) in PBS (pH 7.4).

The P1c concentrations in the liposomes were determined by the bicinchoninic acid (BCA) assay. Briefly, known amount of liposomes were disrupted with methanol, and reacted with the BCA assay reagents according to the manufacturer's instructions. The absorbance of the reaction product was recorded at 562 nm. To determine peptides coupling efficacy, concentrations of P1c were determined before and after dialysis.

The morphological study of the prepared liposomes was carried out with TEM (JEM-1010, JEOL, Japan). The liposomes were dissolved in PBS and dipped on a carbon coated copper grid. The grid was air-dried at room temperature and then imaged with a TEM equipped at 80 kV acceleration voltage.

The DOX concentration in the liposomes was determined by measuring absorption at 480 nm on an ultraviolet-visible spectrometer (UV-2450, Shimadzu, Tokyo, Japan) following liposomes lysis with methanol. To determine DOX encapsulation efficiency (EE), concentrations of DOX were determined

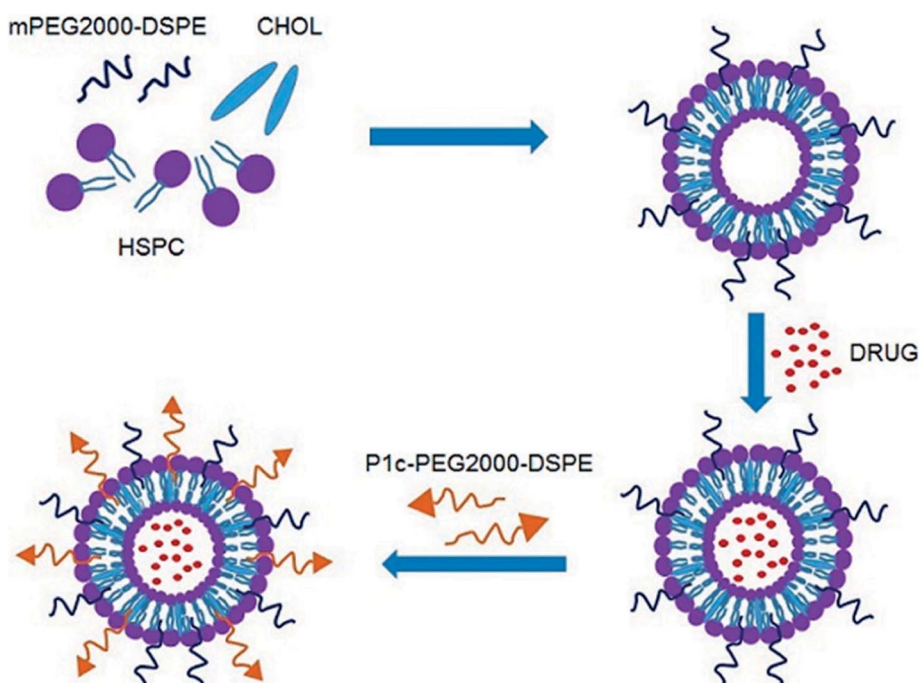


Fig. 1 Schematic representation of P1c-PEG2000-DSPE decorated long circle liposomes.



**Table 1** Particle size, polydispersity index (PDI), zeta potential, encapsulation efficiency (EE) of liposomes

Liposomes	Particle size (nm)	PDI	Zeta potential (mV)	EE (%)
DOXL	128.5 ± 1.6	0.104 ± 0.079	-33.1 ± 1.6	95.7 ± 1.1
P1c-DOXL	131.2 ± 1.8	0.187 ± 0.054	-19.7 ± 2.8	97.5 ± 2.1

before and after dialysis. DOX encapsulation efficiency was calculated by the equation:

$$EE = (\text{DOX concentration after dialysis} / \text{DOX concentration before dialysis}) \times 100\%$$

To evaluate the stability, the liposomes were placed in a refrigerator at 4 °C for one month. The appearance of the liposomes was observed at different time points, and the particle size and DOX release were measured.

### *In vitro* release study

The *in vitro* release kinetics of DOX from the P1c-DOXL was evaluated using a dialysis method. The P1c-DOXL were dispersed in a dialysis membrane bag (MW cut off 8–14 kDa) and the membrane was immersed in a 100 mL beaker

containing 50 mL pH 7.4 PBS buffer in it. The release of DOX from the liposomes was tested under mechanical shaking (150 rpm) at 37 °C. The outer phase of dialysis membrane was withdrawn periodically and the same volume of fresh PBS was complemented. The release DOX was measured by UV-vis spectrophotometry at 485 nm.

### Cell culture

U87MG cells and MCF-7 cells were chosen to test as  $\alpha\beta3$  highly expressed group and negative group, respectively. U87MG cells and MCF-7 cells were cultured in DMEM supplemented with 10% FBS and penicillin (100 U mL<sup>-1</sup>), streptomycin (0.1 mg mL<sup>-1</sup>) at 37 °C in a humidified atmosphere containing 5% CO<sub>2</sub>.

### Determination of $\alpha\beta3$ expression

The expression of integrin  $\alpha\beta3$  in cancer cells was determined by flow cytometry. Briefly, cells were harvested and washed twice with cool PBS containing 1% FBS. The cells were then incubated with anti-human  $\alpha\beta3$  integrin monoclonal antibody (2.5 mg L<sup>-1</sup>, R&D Systems, Minneapolis, MN) in PBS with 1% FBS for 1 hour at 4 °C. A mouse immunoglobulin (Ig) G (R&D Systems, Minneapolis, MN) was used as a negative control. The cells were then washed twice and incubated with goat anti-mouse antibody-FITC (1 mg L<sup>-1</sup>, Santa Cruz, USA) at 4 °C for 30 minutes in the dark. After washed for three times, the cells were resuspended in PBS and analyzed by flow cytometry (Becton Dickinson, San Jose, CA, USA).

### Cellular uptake of DOX

Cellular uptake of DOX was quantified by flow cytometry. Cells were detached using trypsin and suspended in PBS. Free DOX, P1c-DOXL and DOXL were added at equivalent DOX concentration of 4 mg L<sup>-1</sup> and incubated with aliquots of the cells for 1 hour at 37 °C. To confirm the binding of P1c with  $\alpha\beta3$ , cells were preincubated with anti-human  $\alpha\beta3$  integrin monoclonal antibody (0.5 mg L<sup>-1</sup>) for 30 minutes followed by addition of P1c-DOXL. Cells were rinsed with cold PBS three times and

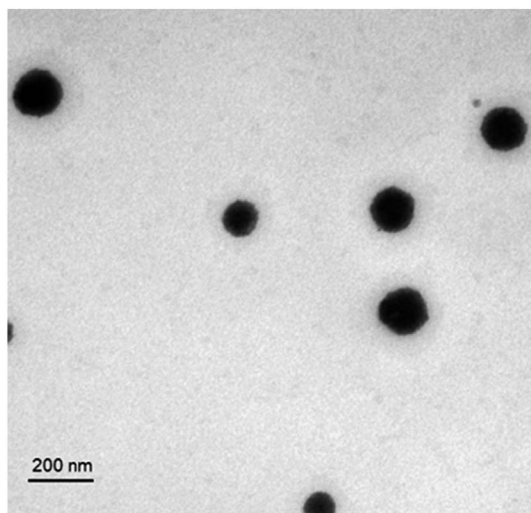


**Fig. 2** TEM picture of P1c-DOXL. The P1c-DOXL exhibited a spherical shape with a diameter of 60–100 nm.

**Table 2** Stability of P1c-DOXL over time

Time (days)	Appearance	DOX release (%)	Particle size (nm)
1	Orange-red homogeneous suspension without delamination and sedimentation	2.5	131.2
10	Orange-red homogeneous suspension without delamination and sedimentation	4.8	138.9
30	Orange-red homogeneous suspension without delamination and sedimentation	18.7	149.3



Table 3 Stability of DOXL over time

Time (days)	Appearance	DOX release (%)	Particle size (nm)
1	Orange-red homogeneous suspension without delamination and sedimentation	4.3	128.4
10	Orange-red homogeneous suspension without delamination and sedimentation	6.4	134.9
30	Orange-red homogeneous suspension without delamination and sedimentation	18.8	143.5

suspended into PBS solution containing 4% formalin before undergoing flow cytometry analysis.

Laser confocal scanning microscope (LCSM) was performed to further investigate cellular uptake of DOX. U87MG and MCF-7 cells were seeded and grown on a 35 mm cell culture dishes for 24 h. Thereafter, the cells were carefully washed with PBS and then incubated with free DOX, P1c-DOXL and DOXL for 1 hour in darkness. The cells were then washed three times with PBS and examined with a LCSM (OLYMPUS-FV1000, Japan). Some U87MG and MCF-7 cells were pre-incubated with 0.5 mg L<sup>-1</sup> anti-human  $\alpha v \beta 3$  monoclonal antibody before the addition of P1c-DOXL for the blocking experiments to determine the bioactivity of P1c.

#### Cytotoxicity assay

The sensitivity of U87MG and MCF-7 cells to DOX was determined by the *in vitro* WST [2-(2-methoxy-4-nitrophenyl)-3-(4-nitrophenyl)-5-(2,4-disulfophenyl)-2H-tetrazolium, monosodium salt] assay. Briefly, 5000 cells were plated in a 96-well plate and incubated overnight. Free DOX, DOXL or P1c-DOXL was then added and incubated for another 48 h. The cellular viability was evaluated using cell counting kit-8 (CCK-8) (Bio Scientific Inc.).

#### Tumor xenografts model

The male BALB/C nude mice (4–6 weeks old) were obtained from the Experimental Animal Center of the Academy of Military Medical Sciences, China, and reared in the Animal Environmental Control Unit. About  $5 \times 10^6$  U87MG cells were subcutaneously inoculated at the right foreleg of nude mice. Tumor volume ( $V$ ) was determined by measuring length ( $a$ ) and

width ( $b$ ), and calculated as  $V = a \times b^2/2$ . When the tumors reached  $\sim 100 \text{ mm}^3$ , the tumor-bearing mice were used for experiments.

#### Antitumor efficacy *in vivo* and toxicological study

Tumor-bearing mice were weighed and randomly divided into four groups ( $n = 6$ ). Free DOX, DOXL or P1c-DOXL was administrated *via* the tail vein on day 0, 3, 6 and 9 at an equivalent dose of 1.5 mg kg<sup>-1</sup> DOX. Saline was used as control. Tumor size and body weight of the tumor-bearing mice were measured every three days. At day 15 post-first drug injection, mice were sacrificed, the tumor tissues were separated and slices were prepared for immunostain for integrin  $\alpha v \beta 3$  and CD31. CD31 is used to demonstrate the presence of endothelial cBCAells to evaluate the degree of tumor angiogenesis. The blood samples were collected and allowed to stand at 4 °C for coagulation. Serum was collected by centrifuging the coagulated blood at 10 000 rpm at 4 °C for 10 min. Serum alanine transaminase (ALT) and aspartate amino transferase (AST) enzyme levels were determined using a commercially available kit (Wako, Nanjing, China) following the manufacturer's instructions. Normal organs including heart, liver, spleen, lung and kidney of the mice were also collected followed by histological evaluation with hematoxylin and eosin (HE) staining.

#### Data processing and statistics

All results were expressed as mean  $\pm$  standard deviation (SD). One-way analysis of variance and student's *t*-test were performed to compare the differences between groups. Values of  $P < 0.05$  were regarded as statistically significant.

## Results and discussion

#### Preparation and characterization of liposomes

As shown in Fig. 1, the P1c-PEG2000-DSPE decorated long circle liposomes were successfully synthesized. The particle sizes of the prepared liposomes were around 130 nm (PDI < 0.2). The DOX encapsulation efficiency (EE) of liposomes was more than 95% (Table 1). TEM was employed to observe the structure of the prepared liposome, which exhibited a uniform spherical shape with a diameter of 60–100 nm (Fig. 2).

A volume of 10 mL liposomes withdrawn and measured with particle size and DOX release at different time points after stored at 4 °C. The DOX release assays were carried out by measuring the DOX present in the outer buffer after dialysis

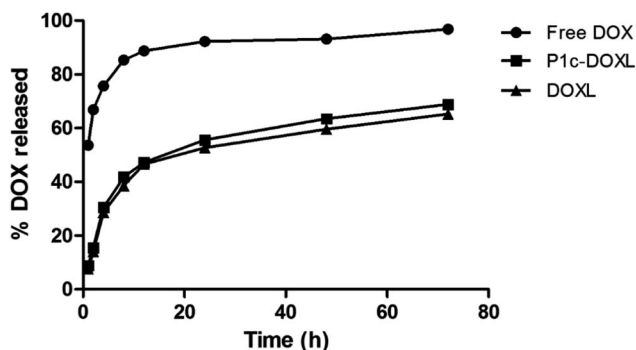


Fig. 3 *In vivo* release curves of free DOX, P1c-DOXL and DOXL.



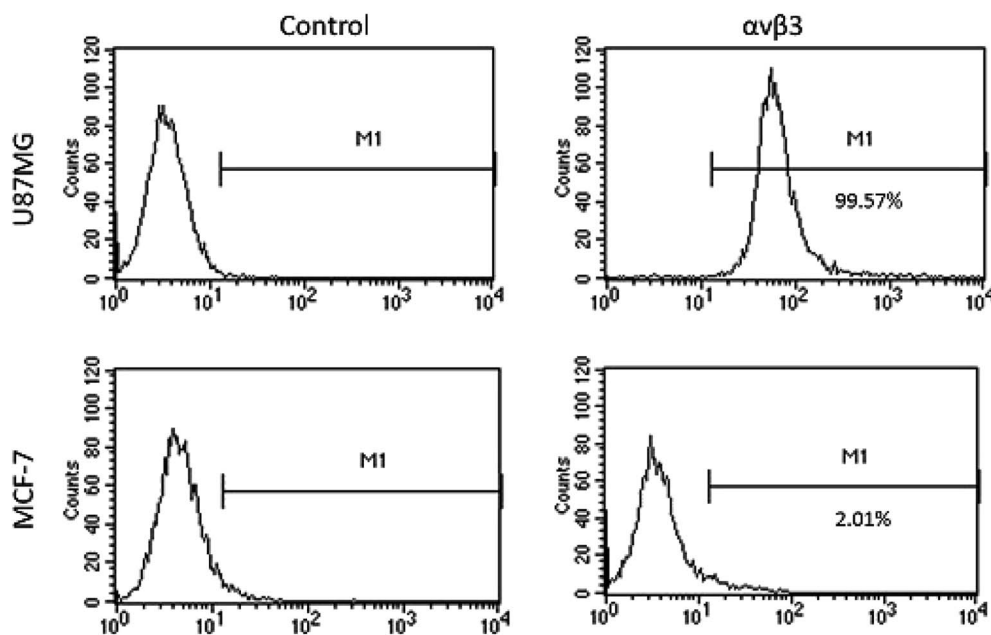


Fig. 4 The expression of integrin  $\alpha\beta3$  on U87MG cells and MCF-7 cells was determined by flow cytometry. A mouse immunoglobulin (Ig) G was used as the negative control.

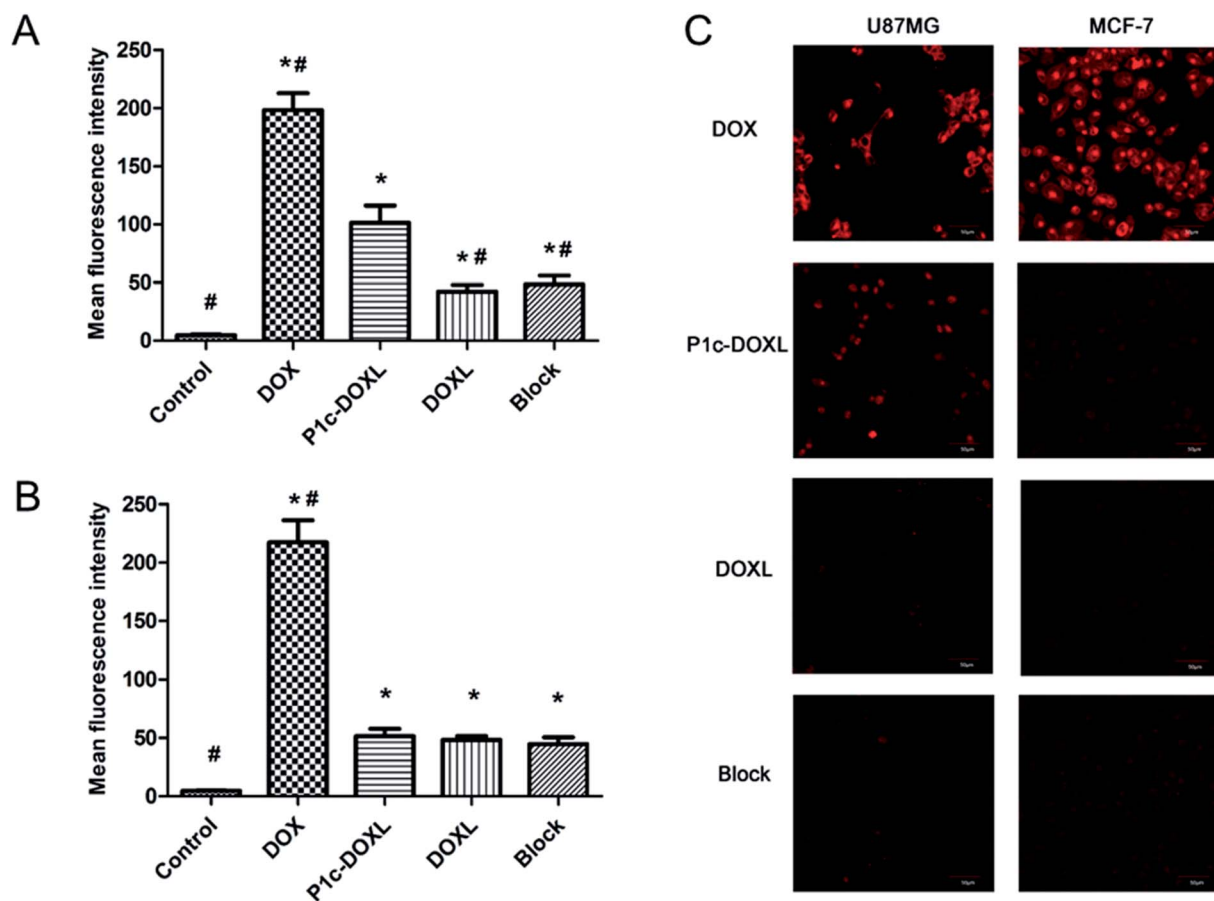


Fig. 5 Cellular uptake of DOX. The mean fluorescence intensity in U87MG (A) and MCF-7 cells (B) by flow cytometry analysis. (C) Cellular uptake of DOX observed by laser confocal scanning microscope (LCSM). Bars indicated of 50  $\mu\text{m}$ . \* vs. control  $P < 0.05$ , # vs. P1c-DOXL  $P < 0.05$ .



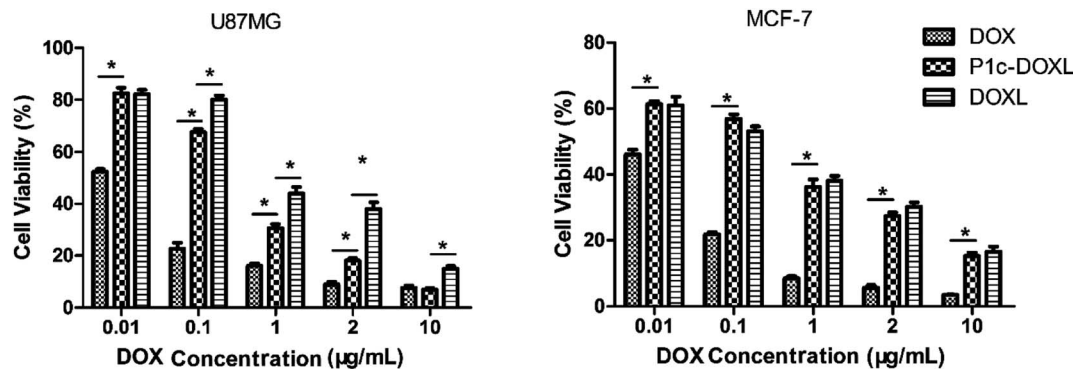


Fig. 6 Cytotoxicity of the prepared liposomes in U87MG and MCF-7 cells. \* $P < 0.05$ .

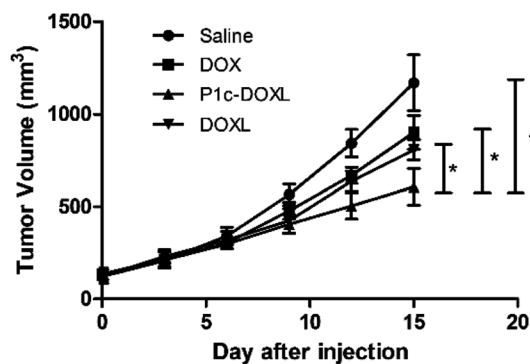


Fig. 7 Therapeutic efficacy of P1c-DOXL in U87MG tumor bearing mice. \* $P < 0.05$ .

against 50 mL pH 7.4 PBS buffer for 8 h. The results shown in Tables 2 & 3 indicated that the prepared liposomes were stable within 10 days without apparent appearance change, DOX release or size degradation.

### Peptide coupling efficacy

P1c coupling efficiency was determined by measuring the P1c concentrations before and after dialysis by BCA assay. Free peptide was removed after extensive dialysis. The P1c peptide coupling efficacy was  $66.8 \pm 1.6\%$ .

### In vitro release study

The drug release rates of free DOX, P1c-DOXL and DOXL into PBS at pH 7.4 and a temperature of  $37^\circ\text{C}$  were shown in Fig. 3. DOX release from the liposomes was characterized with an initial burst release, reaching 45% within the first 12 hours. Then the release became much slower and reached 65% at 72 hours. Compared to the control group, free DOX whose drug release up to 90% within the first 12 hours, the liposomes improved the stability and slowed the sustained release rate of drugs.

### Integrin $\alpha\beta3$ expression on cells

The expression of integrin  $\alpha\beta3$  on U87MG cells and MCF-7 cells was determined by flow cytometry. The positively expression rate of  $\alpha\beta3$  was about 99% in U87MG cells, while it is 2.01% for MCF-7 cells (Fig. 4).

### In vitro cellular uptake study

Cellular uptake of DOX is shown in Fig. 2. U87MG and MCF-7 cells were treated with free DOX, P1c-DOXL and DOXL at an equivalent concentration of  $4 \mu\text{g mL}^{-1}$  DOX for 1 h. Fig. 2A showed the mean fluorescence intensity in U87MG cells by flow cytometry analysis. Compared to DOXL, P1c-DOXL showed greater uptake by U87MG cells ( $P < 0.05$ ), which demonstrated that P1c coupling lead to increased cellular uptake of liposomes. Additionally, the cellular uptake of P1c-DOXL decreased when U87MG cells were pre-incubated with anti- $\alpha\beta3$  monoclonal antibody as shown in the block group. The phenomenon implied anti- $\alpha\beta3$  monoclonal antibody competed with P1c-DOXL for  $\alpha\beta3$  docking sites. As shown in Fig. 2B, there was no significant differences between the P1c-DOXL and DOXL groups in MCF-7 cells ( $P > 0.05$ ). The free DOX showed the highest cellular uptake in both cell lines (Fig. 5A and B).

Laser confocal scanning microscope (LCSM) was also performed to investigate cellular uptake of liposomes. Fig. 2C showed that greater fluorescence intensity was observed in U87MG cells treated with P1c-DOXL group compared to DOXL group or mAb-blocking group. MCF-7 cells (Fig. 5C) were much less attractive for P1c-DOXL. These results agreed with that of flow cytometry analysis. Such results suggested that cellular uptake of the DOX was enhanced by the specific interaction between P1c and  $\alpha\beta3$  on the surface of integrin-rich U87MG cells.

### In vitro cytotoxicity study

The cytotoxicity of the liposomes in U87MG and MCF-7 cells was evaluated using the CCK-8 assay (Fig. 6). Cells were incubated with free DOX, DOXL, or P1c-DOXL for 48 h, and the cell viability was investigated.

In both U87MG and MCF-7 cells, free DOX demonstrated the highest cytotoxicity. In U87MG cells, P1c-DOXL showed higher



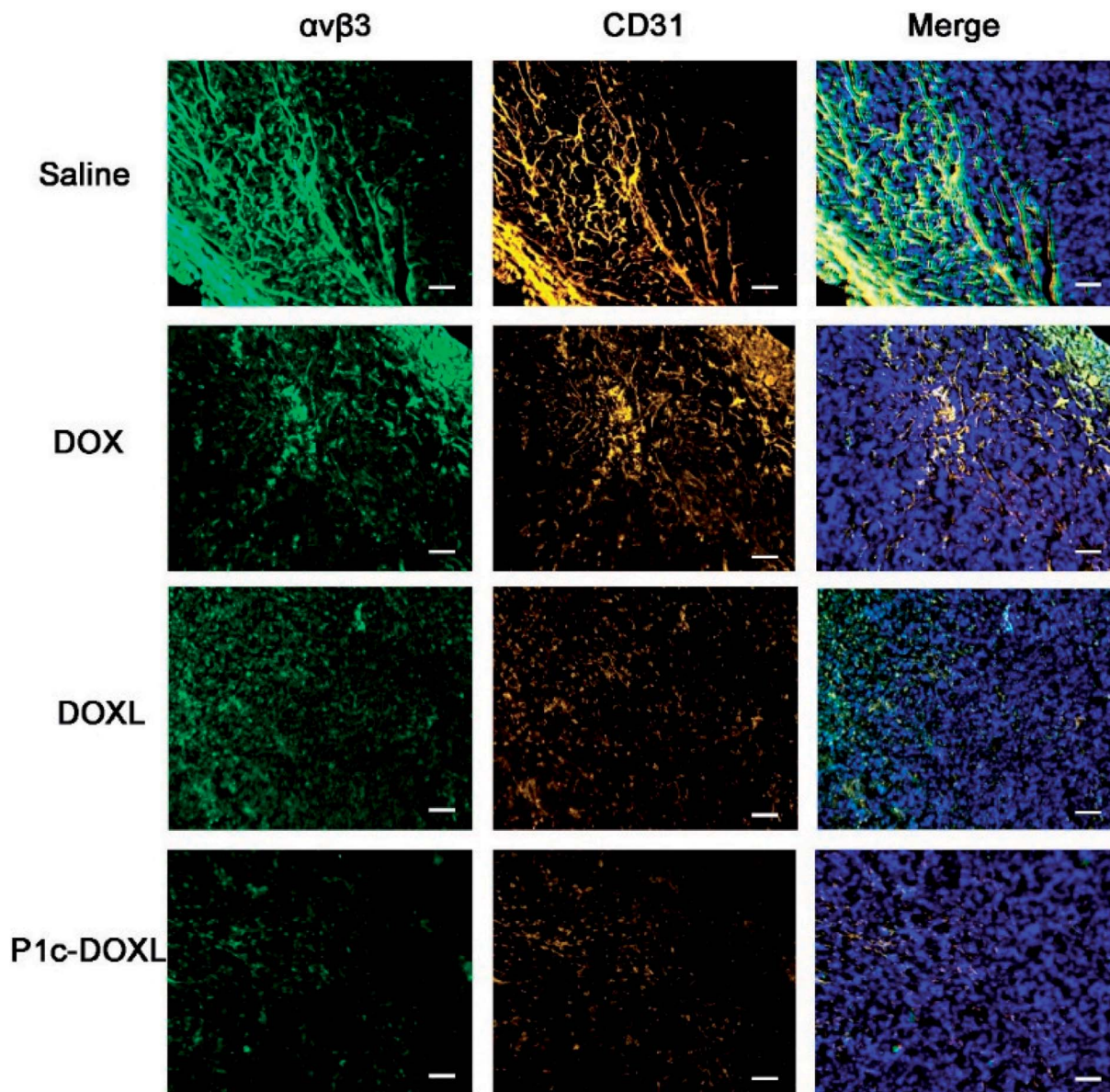


Fig. 8 Immunofluorescence analysis for integrin  $\alpha v \beta 3$  (green) and CD31 (orange) in tumor tissues. Nuclei were detected with DAPI (blue). Scale bars, 50  $\mu\text{m}$ .

cytotoxicity (*i.e.* lower  $\text{IC}_{50}$ ) than DOXL liposomes. The  $\text{IC}_{50}$  values were 0.24 and 0.7  $\mu\text{g mL}^{-1}$  for P1c-DOXL and DOXL liposomes, respectively. In MCF-7 cells which were negatively expressing  $\alpha v \beta 3$ , there was no significant differences between the P1c-DOXL and DOXL liposomes. Improved cytotoxicity for the P1c-DOXL in U87MG may be attributed to the specific targeting of P1c as shown in the results of cellular uptake assay (Fig. 5).

#### *In vivo* antitumor efficacy

The *in vivo* therapeutic efficacy of P1c-DOXL and DOXL were evaluated in U87MG tumor engrafted mouse model. As shown in Fig. 7, compared with saline, DOX, and DOXL groups, P1c-DOXL dramatically reduced tumor growth ( $P < 0.05$ ). The

results from immunofluorescence analysis (Fig. 8) showed that both the expression of integrin  $\alpha v \beta 3$  and CD31 of the P1c-DOXL group were lowest compared to treatment with non-targeting liposome (DOXL) and DOX groups implying the anti-angiogenesis activity of the P1c-modified targeting liposomes.

#### *In vivo* toxicity

After three times of injection of DOX, the mice showed remarkable decrease of body weights (Fig. 9), and one died at day 14. There was no significant body weight loss in saline or liposome groups (Fig. 9A). Histological evaluation showed that compared to saline and liposome groups, DOX have notable hepatotoxicity as shown in Fig. 9B. No unusual changes in the heart, liver, spleen, lung and kidney were observed (Fig. 9C–F)



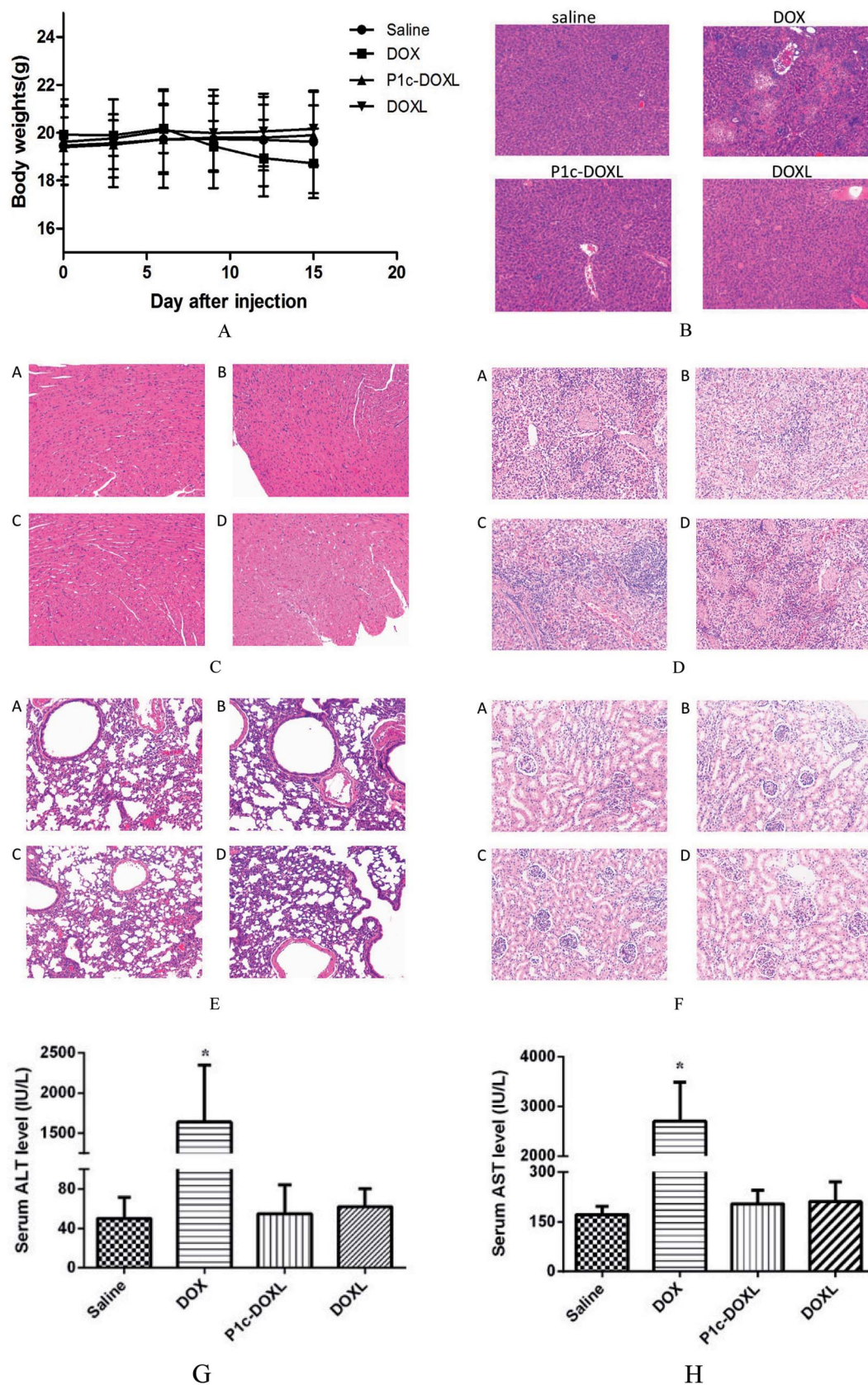


Fig. 9 The *in vivo* cytotoxicity of the prepared liposomes. (A) Body weights of U87MG tumor bearing mice after injection of drugs. (B) Histological evaluation of livers of the U87MG tumor bearing mice after injection of drugs. (C–F) Histological evaluation of heart, spleen, lung and kidney of the U87MG tumor bearing mice after injection of drugs, respectively. (G & H) Hepatotoxicity of the prepared liposomes. Blood sample was collected and toxicological study was performed by measuring the serum ALT and AST level.\* vs. saline  $P < 0.05$ .



in all groups. Additionally, as markers for hepatotoxicity, the serum ALT and AST enzyme levels of mice were also measured (Fig. 9G & H) and exhibit the highest enzymes levels in DOX group, while no significant difference was observed in the other groups in comparison with the saline group. These results all indicated that the liposomes had superior *in vivo* security.

## Conclusions

P1c-modified targeting liposomes exhibiting sustained release, enhanced the antitumor effect of DOX through targeting tumor cells and neovascular where integrin  $\alpha v\beta 3$  was overexpressed. The results indicated that the P1c-modified drug delivery system might be a promising solution for active targeting delivery.

## Ethical statement

All procedures involving animals and their care were conducted in conformity with NIH guidelines (NIH Pub. no. 85-23, revised 1996) and was approved by Animal Care and Use Committee of the Southeast University and Ethics Committee of Southeast University (Nanjing, China).

## Conflicts of interest

The authors have declared that no competing interests exists.

## Acknowledgements

The work was supported by the National Science and Technology Major Project of China (No. 2018ZX09301026-005), National Natural Science Foundation of China (No. 81603016 & 81773624), Project of Social Development of Jiangsu Province (No. BE2017746 & BK.20160706). We kindly appreciate Prof. Liu Yu from China Pharmaceutical University for help with the liposomes preparation.

## References

- 1 V. P. Torchilin, *Nat. Rev. Drug Discovery*, 2005, **4**, 145–160.
- 2 S. Zununi Vahed, R. Salehi, S. Davaran and S. Sharifi, *Mater. Sci. Eng., C*, 2017, **71**, 1327–1341.
- 3 A. Laouini, C. Charcosset, H. Fessi, R. G. Holdich and G. T. Vladisavljevic, *Colloids Surf., B*, 2013, **112**, 272–278.
- 4 M. Barattin, A. Mattarei, A. Balasso, C. Paradisi, L. Cantù, E. D. Favero, T. Viitala, F. Mastrotto, P. Caliceti and S. Salmaso, *ACS Appl. Mater. Interfaces*, 2018, **10**, 17646–17661.
- 5 T. M. Allen, *Trends Pharmacol. Sci.*, 1994, **15**, 215–220.
- 6 F. Yuan, M. Leunig, S. K. Huang, D. A. Berk, D. Papahadjopoulos and R. K. Jain, *Cancer Res.*, 1994, **54**, 3352–3356.
- 7 H. Maeda, *Adv. Enzyme Regul.*, 2001, **41**, 189–207.
- 8 N. Naziris, N. Pippa, A. Meristoudi, S. Pispas and C. Demetzos, *J. Liposome Res.*, 2016, **27**, 1.
- 9 Q. Yao, H. Chen, W. Yuan, K. Rui, Q. Zhang, F. Xie, Z. Li, Z. Zhang, L. Ji and H. Qin, *Int. J. Pharm.*, 2011, **419**, 85.
- 10 H. I. Labouta, M. J. Gomez-Garcia, C. D. Sarsons, T. Nguyen, J. Kennard, W. Ngo, K. Terefe, N. Iragorri, P. Lai, K. D. Rinker and D. T. Cramb, *RSC Adv.*, 2018, **8**, 7697–7708.
- 11 L. Zhang, A. A. Habib and D. Zhao, *Oncotarget*, 2016, **7**, 38693–38706.
- 12 W. Kang, D. Svirskis, V. Sarojini, A. L. McGregor, J. Bevit and Z. Wu, *Oncotarget*, 2017, **8**, 36614–36627.
- 13 Z. Chen, J. Deng, Y. Zhao and T. Tao, *Int. J. Nanomed.*, 2012, **7**, 3803–3811.
- 14 G. Xiang, J. Wu, Y. Lu, Z. Liu and R. J. Lee, *Int. J. Pharm.*, 2008, **356**, 29–36.
- 15 Y. Chen, V. Minh le, J. Liu, B. Angelov, M. Drechsler, V. M. Garamus, R. Willumeit-Romer and A. Zou, *Colloids Surf., B*, 2016, **140**, 74–82.
- 16 X. Li, L. Ding, Y. Xu, Y. Wang and Q. Ping, *Int. J. Pharm.*, 2009, **373**, 116–123.
- 17 X. L. Song, S. Liu, Y. Jiang, L. Y. Gu, Y. Xiao, X. Wang, L. Cheng and X. T. Li, *Eur. J. Pharm. Sci.*, 2017, **96**, 129–140.
- 18 E. Ruoslahti and M. D. Pierschbacher, *Science*, 1987, **238**, 491.
- 19 R. O. Hynes, *Cell*, 1992, **69**, 11–25.
- 20 G. Gasparini, P. C. Brooks, E. Biganzoli, P. B. Vermeulen, E. Bonoldi, L. Y. Dirix, G. Ranieri, R. Miceli and D. A. Cheresch, *Clin. Cancer Res.*, 1998, **4**, 2625–2634.
- 21 L. Bello, M. Francolini, P. Marthyn, J. Zhang, R. S. Carroll, D. C. Nikas, J. F. Strasser, R. Villani, D. A. Cheresch and P. M. Black, *Neurosurgery*, 2001, **49**, 380–389.
- 22 A. V. Wallbrunn, C. Hölteke, M. Zühlendorf, W. Heindel, M. Schäfers and C. Bremer, *Eur. J. Nucl. Med. Mol. Imaging*, 2007, **34**, 745–754.
- 23 H. Wu, H. Chen, Y. Sun, Y. Wan, F. Wang, B. Jia and X. Su, *Cancer Lett.*, 2013, **335**, 75–80.
- 24 J. D. Robertson, J. R. Ward, M. Avila-Olias, G. Battaglia and S. A. Renshaw, *J. Immunol.*, 2017, **198**, 3596–3604.
- 25 F. Wang, L. Chen, R. Zhang, Z. Chen and L. Zhu, *J. Controlled Release*, 2014, **196**, 222–233.
- 26 B. M. Dicheva, T. L. ten Hagen, A. L. Seynhaeve, M. Amin, A. M. Eggermont and G. A. Koning, *Pharm. Res.*, 2015, **32**, 3862–3876.
- 27 W. T. Chen, T. T. Shih, R. C. Chen, S. Y. Tu, W. Y. Hsieh and P. C. Yang, *Mol. Imaging*, 2012, **11**, 286–300.
- 28 J. S. Desgrosellier and D. A. Cheresch, *Nat. Rev. Cancer*, 2010, **10**, 9.
- 29 G. Wu, X. Wang, G. Deng, L. Wu, S. Ju, G. Teng, Y. Yao, X. Wang and N. Liu, *J. Magn. Reson. Imaging*, 2011, **34**, 395–402.

